ACS APPLIED MATERIALS & INTERFACES

Research Article

www.acsami.org

Encapsulating Ionic Liquid and Fe_3O_4 Nanoparticles in Gelatin Microcapsules as Microwave Susceptible Agent for MR Imaging-guided Tumor Thermotherapy

Qijun Du,[†,‡,§] Tengchuang Ma,[†,⊥] Changhui Fu,[‡] Tianlong Liu,[‡] Zhongbing Huang,*[,§] Jun Ren,[‡] Haibo Shao,*[,⊥] Ke Xu,[⊥] Fangqiong Tang,[‡] and Xianwei Meng*[,‡]

[‡]Laboratory of Controllable Preparation and Application of Nanomaterials, Center for Micro/nanomaterials and Technology, Technical Institute of Physics and Chemistry, Chinese Academy of Sciences, Beijing 100190, China

[§]College of Materials Science and Engineering, Sichuan University, Chengdu 610065, China

[⊥]Department of Radiology, First Hospital of China Medical University, Shenyang 110001, China

Supporting Information

ABSTRACT: The combination of therapies and monitoring the treatment process has become a new concept in cancer therapy. Herein, gelatin-based microcapsules have been first reported to be used as microwave (MW) susceptible agent and magnetic resonance (MR) imaging contrast agent for cancer MW thermotherapy. Using the simple coacervation methods, ionic liquid (IL) and Fe_3O_4 nanoparticles (NPs) were wrapped in microcapsules, and these microcapsules showed good heating efficacy in vitro under MW irradiation. The results of cell tests indicated that gelatin/IL@Fe_3O_4 microcapsules possessed excellent compatibility in physiological environments, and they could effectively kill cancer cells with exposure to MW. The ICR mice bearing H22 tumors treated with gelatin/IL@Fe_3O_4 microcapsules were obtained an outstanding MW thermotherapy efficacy with 100% tumor elimination under ultralow density irradiation (1.8 W/cm^2, 450 MHz). In addition, the applicability of the microcapsules as an efficient contrast agent for MR imaging in vivo was evident. Therefore, these multifunctional microcapsules have a great potential for MR imaging-guided MW thermotherapy.

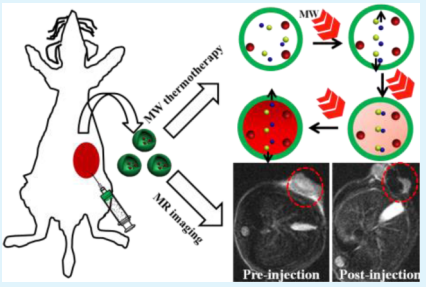

KEYWORDS: *MW thermotherapy, tumor, gelatin microcapsules, MR imaging-guided, ionic liquid*

INTRODUCTION

The statistical analysis showed a high rate of cancer incidence and mortality in the worldwide. Surgery is an optimal treatment for early stage cancer; however, many patients are unsuitable for surgical treatment because of the appearance of multiple tumors, metastases at other sites, or unfavorable tumor location.[1−4] Many minimally invasive technologies have been developed for alternate treatment modalities.[5−8] Microwave (MW) thermotherapy, one of the most promising options for patients with unresectable tumors,[9,10] could induce the tumor destruction using the heat produced by dielectric hysteresis.[11−14] Under the irradiation of MW, the intracellular water molecules polarize and oscillate at a frequency of billions times per second, resulting in the heating of tissue.[15−18] The benefits of MW thermotherapy are very short heating time, effective large tumor ablation, consistently high intratumoral temperature, and a less heat sink effect.[19−24] The materials with specific MW absorption and generating additional heat such as carbon compounds and ferrite,[25−32] can offer the potential for improving the efficacy and safety of MW thermotherapy. Recently, microcapsules with a core of saline as microwave-susceptible agents for tumor MW thermotherapy in an animal model have been developed,[33,34] and Na^+ and Cl^- ions inside the microcapsules exhibited higher microwave susceptible properties than free saline because of the spatial confinement efficiency of microcapsule walls. Despite the microcapsules filled with saline have been accepted as an effective microwave susceptible agent, there are still many challenges ahead toward further clinical applications of those microcapsules in MW thermotherapy of cancer. One of the most important issues is uncontrollable thermal distribution during the MW thermotherapy process, which leads to not only high recurrence rate but also damage of adjacent vital organs. It is highly desirable to create novel imaging-guided MW susceptible agent to real-time monitor the course of therapy for the optimization of therapeutic outcome.

Herein, MR imaging-guided MW thermotherapy is achieved in vivo for the first time by the microcapsules, which are composed of ionic liquids (IL) and Fe_3O_4 NPs as the core and polymer materials (gelatin) as the shell (designated as gelatin/IL@Fe_3O_4). IL encapsulated in microcapsules is developed for MW tumor thermotherapy. With the characteristics of ionic

Received: April 14, 2015
Accepted: June 2, 2015
Published: June 2, 2015

DOI: 10.1021/acsami.5b03230
ACS Appl. Mater. Interfaces 2015, 7, 13612−13619

character and high polarizability, IL show highly susceptible to MW irradiation.[35−40] The strongly MW absorbing property makes IL high potential for MW treatment of cancer cell. The MR imaging modality, Fe_3O_4 NPs, in the microcapsule is designed to monitor the tumor response after the MW irradiation, assess the therapeutic treatment efficacy, and reduce side effects to nearby normal tissues. High-efficiency MW thermotherapy of ICR mice bearing H22 tumors in vivo is achieved, realizing 100% of tumor elimination with a moderate dose of the MW susceptible agent under low density of MW irradiation (1.8 W/cm^2, 450 MHz, 5 min). Moreover, using gelatin/IL@Fe_3O_4 microcapsules as an MR imaging probe is also proven. It can be noted that the combination of IL and MW thermotherapy opens the door to interesting opportunities broadly in IL applications and tumor therapeutics.

EXPERIMENTAL METHODS

Materials. All chemicals were used as received in this work without further purification. Ferric chloride hexahydrate ($FeCl_3·6H_2O$), sodium acetate (NaAc), ethylene glycol and sodium citrate were obtained from Sinopharm Chemical Reagent Beijing Co., Ltd. Gelatin (Mw = 100000) was purchased from Sigma-Aldrich. Soybean oil was purchased from Beijing Guchuan Oil Co. Span 80 and glutaraldehyde (GA) were obtained from Institute of Tianjin Jinke Fine Chemicals. 1-Butyl-3-methylimidazolium tetrafluoroborate (composed solely of ions yet are liquid at room temperature, designated as IL) was purchased from Shanghai Chengjie Chemical Co., Ltd. Hematoxylin and eosin (H&E stain) were obtained from Beijing Solarbio Science &Technology Co. (China).

Synthesis of Gelatin/IL Microcapsules. Gelatin (0.65 g) was completely dissolved in 5 mL of 4% IL solution at 40 °C to form the water phase. The oil phase was formed by 50 mL soybean oil and 1.2 mL Span 80. Then water phase was added drop by drop into above oil phase under vigorous stirring for 15 min. At last, 1.5 mL of 50% cross-linking agent (GA) was added and the mixture was vigorously stirred for 60 min below 10 °C. The product was obtained after washing several times with isopropyl alcohol and water, respectively, and dried at room temperature.

Synthesis of Gelatin/IL@Fe_3O_4 Microcapsules. The synthesis of Fe_3O_4 NPs was carried out by a simple solvothermal approach. In a typical process, 1.4 g of $FeCl_3·6H_2O$ and 1.0 g of sodium citrate were dissolved in ethylene glycol (30 mL) under stirring for 10 h to form a yellow brown solution and recorded as solution A. Two and four-tenths of a gram of NaAc was completely dissolved in ethylene glycol (10 mL) under stirring and recorded as solution B. Then, solution A and solution B were mixed together under vigorous stirring for 1 h. The obtained suspension was then transferred to 50 mL Teflonlined stainless steel autoclave and heated at 200 °C for 10 h. After the solution was cooled to room temperature, the black precipitates (Fe_3O_4 NPs) were separated by a magnet. The obtained precipitates were washed several times with deionized water and absolute ethanol, respectively, and then dried at room temperature. To obtain gelatin/IL@Fe_3O_4 microcapsules, 0.02 g of Fe_3O_4 was added into gelatin/IL microcapsules during the gelatin dissolve process.

Characterization. Scanning electron microscopy (SEM, S-4300, Hitachi) was used to characterize the morphology of synthesized microcapsules. Energy-dispersive spectroscopy (EDS) coupled with Hitachi S-4800 SEM was used to analyze the element composition of the samples. Fourier transform infrared spectrometry (FT-IR, Varian, Model 3100 Excalibur) was employed to characterize the surface functional groups of the microcapsules. The thermal properties of the microcapsules were measured by thermogravimetric analysis (TG, ICES-001, Canadian) in the temperature range from room temperature to 800 °C with a heating rate of 10 °C per minute in nitrogen atmosphere. X-ray diffraction patterns (XRD) of the as-synthesized samples were analyzed with graphite monochromatised Cu Kα radiation (λ = 1.5148 Å, Japan,) on a Japan Rigaku D/max γA X-ray diffractometer. The tumor photographs were obtained with a Canon DS126231 digital camera. UV/vis spectra were performed by using a spectrophotometer (JASCO V-570) at room temperature. The magnetic hysteresis loops of the as-prepared microcapsules were investigated by a magnetometer (model PPMS-9).

In Vitro MW Heating Experiment. To evaluate the as-prepared microcapsules hyperthermia efficacy under MW irradiation in vitro, the samples were exposed to MW for 5 min. The as-prepared microcapsules were dispersed in saline to obtain 50 mg/mL of solution. The as-prepared Fe_3O_4 NPs were dispersed in water to obtain 50 mg/mL of solution. One mL as-prepared samples solution was added into a 12-well plate with a thin bottom. Then the solutions were exposed to MW (1.8 W/cm^2, 450 MHz, Beijing Muheyu Electronics Co., LTD) irradiation. The temperature of the solution was recorded every 10 s with fiber thermometers (Beijing Dongfangruizhe Technology Co., LTD) and infrared thermal mapping apparatus (FLIR SC620), respectively.

Blood Compatibility Studies. Rabbit's heart blood was used to evaluate the compatibility of the as-prepared microcapsules. Rabbit's red blood cells (RBC) were separated from fresh EDTA-stabilized rabbit's heart blood by centrifugation and washed with PBS for three times, and then diluted with PBS solution to obtain 2% RBC. 0.5 mL RBC suspensions were slowly added into 0.5 mL gelatin/IL@Fe_3O_4 microcapsules in PBS. Then, the samples were mildly mixed and then kept at room temperature for 3 h. Distilled water and a PBS solution were used as positive control (100% lysis) and negative control (0% lysis), respectively. The absorbance of the supernatant was determined at 570 nm by an ultraviolet spectrophotometer. The hemolysis rate (%) was determined as followed: hemolysis rate % = (tested sample-negative control)/ (positive control − negative control) × 100. Less than 5% hemolysis rate was regarded as a nontoxic effect level in this experiment. All experiments were repeated triplicate.

Cell Viability Test in Vitro by MTT Assays. MTT assays of the HepG2 cell line were used to evaluate the potential cytotoxicity of as-prepared microcapsules. A total of 100 μL of HepG2 cells were seeded onto 96-well plates at an initial concentration of approximately 4 × 10^4 cells/mL, and then incubated for 24 h with culture conditions. Different concentrations of gelatin/IL@Fe_3O_4 microcapsules (diluted in DMEM medium) were added into the wells, respectively, and cells were cultured at 37 °C for 24 h. The control group was only HepG2 cells without microcapsules. In order to obtain the results of MTT assay, 20 μL MTT-phosphate saline-buffered solution (PBS) solutions were added into each well and the plate was incubation at 37 °C for another 4 h. Then, 150 μL DMSO was added into wells after the medium was removed. The absorbance at 492 nm was measured with a scanning multiwall spectrometer (Multiskan MK3 Thermo). The cell viability (%) = (absorbance of experimental)/(absorbance of control groups). All of the experiments were designed for five repeating groups.

Cell Viability Test under MW Irradiation. For in vitro studying the microcapsules sensitizing effect on cells, we mixed 500 μL of HepG2 cells suspension (4 × 10^4 cells/mL) with 500 μL of gelatin/IL@Fe_3O_4 microcapsules (dispersed in DMEM medium, 1000 μg/mL). The cells were then irradiated by MW (1.8 W/cm^2, 450 MHz) for 5 min and further incubated for another 24 h. Fiber thermometers were used to record the temperature change of the cells. The MW group was only treated with MW irradiation without microcapsules (MW only), and the control group was without any treatment (control). Finally, the cell viabilities were evaluated by MTT assay.

In Vivo MW Heating Experiment. Twenty female ICR mice (~22 g, 6 weeks) bearing H22 tumor (~300 mm^3) in the axillary region were randomly divided into four groups including untreated mice (Control), MW treated mice with saline, gelatin/IL@Fe_3O_4 microcapsules injected mice with MW irradiation, gelatin/IL@Fe_3O_4 microcapsules injected mice without MW irradiation. The treatment mice groups were intratumoral injected with microcapsules (200 mg/kg), respectively. After 1h injection, mice were anesthetized with sodium pentobarbital, and then the tumor in mice was irradiated with MW (450 MHz, 1.8 W/cm^2) for 5 min. Tumor sizes and body weights were measured every 3 days during the treatment. The tumor sizes were calculated as the volume (V) = (length)(width)^2/2. Relative

DOI: 10.1021/acsami.5b03230
ACS Appl. Mater. Interfaces 2015, 7, 13612−13619

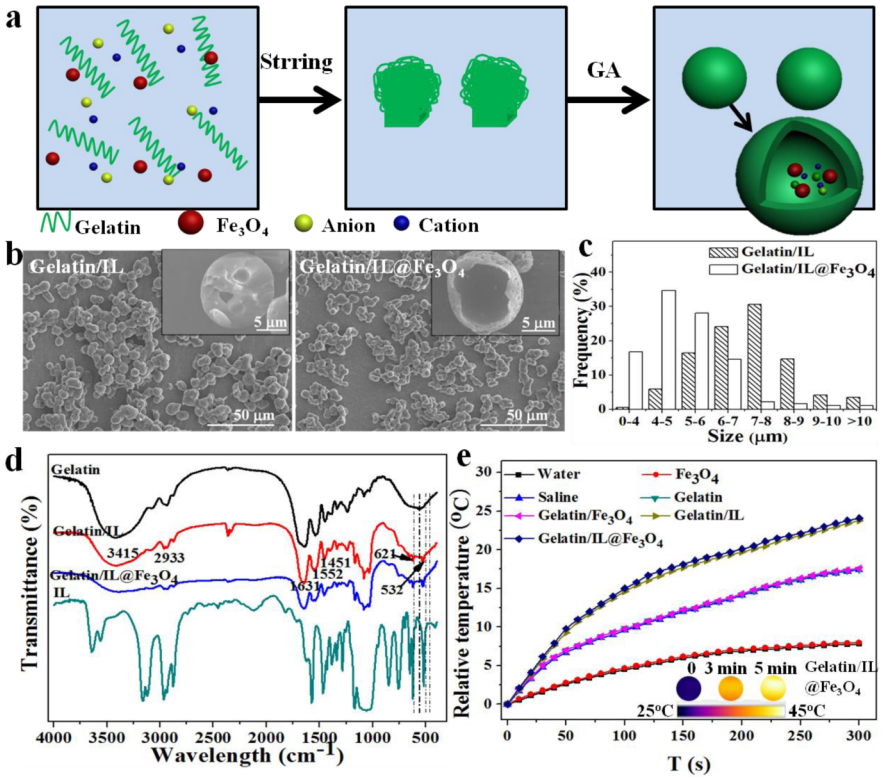

Figure 1. Microcapsule synthesis and characterization. (a) Schematic diagram for the fabrication of gelatin/IL@Fe_3O_4 microcapsules. (b) SEM images of gelatin/IL and gelatin/IL@Fe_3O_4 microcapsules. Inset: cross-section of microcapsule. (c) Size distribution of gelatin/IL and gelatin/IL@Fe_3O_4 microcapsules based on statistical analysis results were determined by a panel of more than 200 microcapsules in b. (d) FT-IR spectra of gelatin, gelatin/IL, gelatin/IL@Fe_3O_4 microcapsules, and IL. (e) MW heating curves of pure water, Fe_3O_4, saline, gelatin, gelatin/Fe_3O_4, gelatin/IL, and gelatin/IL@Fe_3O_4 microcapsules (1 mL, 50 mg/mL) under 450 MHz MW irradiation at the power density of 1.8 W/cm^2. Inset: IR thermal image of gelatin/IL@Fe_3O_4 microcapsules after MW irradiation at 1.8 W/cm^2 for 5 min.

tumor volumes were calculated as V/V_0, where V_0 is the tumor volume when the treatment was initiated. Relative body weight was calculated as $m - m_0$, where m_0 is the body weight when the treatment was initiated. All animal experiments in this work were performed in accordance with the guidelines of the Institutional Animal Care.

Histological Study of Tissues. After 17 days of therapy, the tissues and organs, including liver, heart, spleen, lung, kidney and tumor tissues were excised. The tumor tissues were weighed. Tissues recovered from the necropsy were fixed in 10% formalin, embedded in paraffin, sectioned, and stained with hematoxylin and eosin (HE) for histological examination using standard techniques. The sections of tissues were observed using optical fluorescence microscope (Nikon Eclipse Ti−S, CCD: Ri1).

MR Imaging. MR images and relaxation time measurements were performed with a 3.0 T magnetic resonance system at room temperature (Signa HDx; General Electric Medical Systems, USA). The samples were first dispersed in water with various gelatin/IL@Fe_3O_4 microcapsules concentrations (0.25, 0.5, 1, 2, 6 mg/mL), respectively. The T_2 values and T_2-weighted images were obtained by the same multislice multiecho sequence. MR images were taken before and after the intratumoral injection of gelatin/IL@Fe_3O_4 microcapsules (200 mg/kg). Relaxivity values of r_2 were calculated through the curve fitting of $1/T_2$ relaxation time versus the microcapsules concentration.

Statistical Analysis. The results were represented by average ± standard deviation. The statistical significance of the changes between tested groups and the control group were analyzed by one way ANOVA using SPSS 17.0.

RESULTS AND DISCUSSION

A simple and efficient route is first developed for the fabrication of gelatin/IL@Fe_3O_4 microcapsules. The microcapsules are composed of Fe_3O_4 NPs and IL as the core, and gelatin as the outer (Figure 1a). This coacervation route involves two steps, including the initial fabrication of the Fe_3O_4 NPs and polymer microcapsules via cross-link. Amino group in gelatin can be reacted carboxyl groups in GA to from compounds.[41] The morphology nature of the microcapsules obtained from simple coacervation methods were characterized by SEM. As shown in Figure 1b, gelatin/IL and gelatin/IL@Fe_3O_4 microcapsules were not coalesced and remained good individual spherical shape, and the inserted image indicated that these microcapsules have hollow structure. To evaluate the size distribution of the as-prepared microcapsules, more than 200 particles were measured in Figure 1b, and the statistic result was presented in Figure 1c, indicating that the average sizes of gelatin/IL and gelatin/IL@Fe_3O_4 microcapsules are 7.03 and 5.05 μm, respectively.

The chemical composition of the obtained microcapsules was investigated by FT-IR, EDS, XRD and TG. Figure 1d showed the FT-IR spectra of gelatin, gelatin/IL, gelatin/IL@Fe_3O_4 microcapsules and IL. It was clear that gelatin/IL and gelatin/IL@Fe_3O_4 microcapsules had additional peaks. The peaks at 621 and 532 cm^{-1} are assigned to out-plane C−H bending vibrations of imidazolium ring,[42,43] suggesting the presence of IL. Besides the C, N, and O from the microcapsules, the peak of F was detected in the EDS pattern of gelatin/IL and gelatin/IL@Fe_3O_4 microcapsules (Figure S1a, b in the Supporting Information). Fe element was observed in the gelatin/IL@Fe_3O_4 microcapsules (Figure S1c). The XRD patterns of as-prepared microcapsules and Fe_3O_4 NPs (Figure

DOI: 10.1021/acsami.5b03230
ACS Appl. Mater. Interfaces 2015, 7, 13612−13619

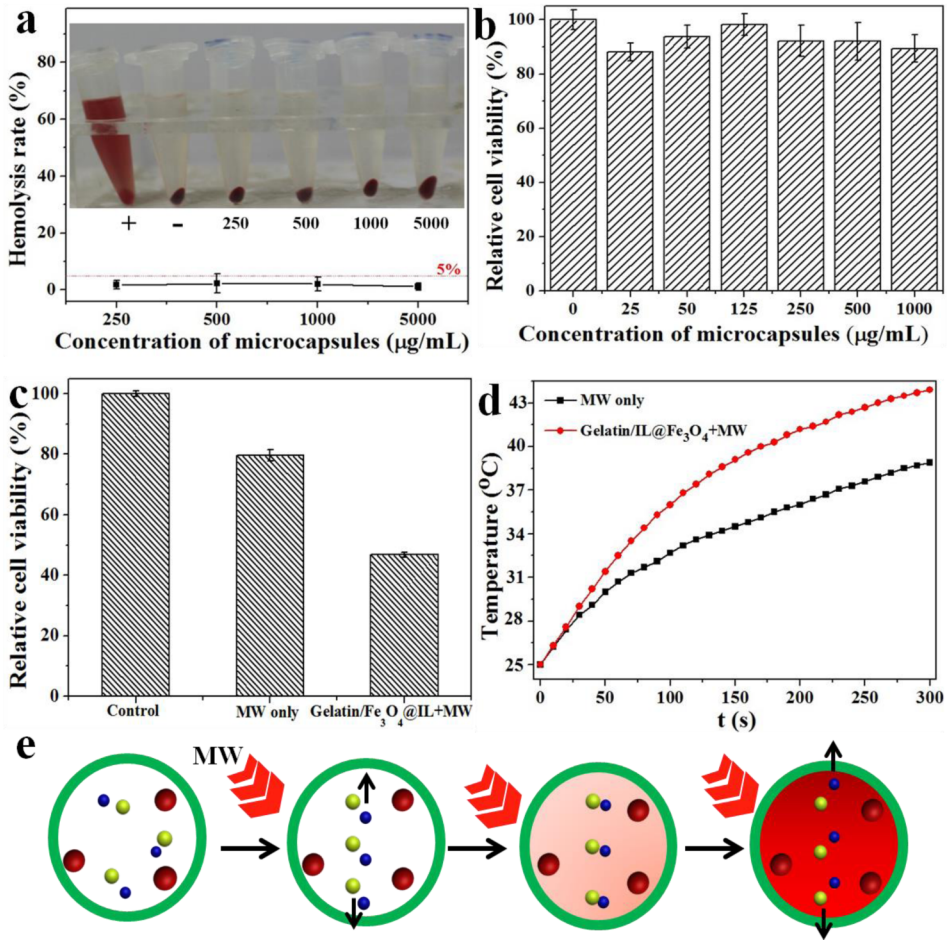

Figure 2. In vitro cell experiments. (a) Hemolysis rate of red blood cells incubated with gelatin/IL@Fe_3O_4 microcapsules at various concentrations for 3 h, using deionized water (+) and PBS (−) as positive and negative controls, respectively. Inset: Photographs of hemolysis test with different concentrations of gelatin/IL@Fe_3O_4 microcapsules. (b) Cell viability of HepG2 cells incubated with gelatin/IL@Fe_3O_4 microcapsules of different concentrations for 24 h. (c) Viability of HepG2 cells after being mixed with gelatin/IL@Fe_3O_4 microcapsules under MW irradiation (450 MHz, 1.8 W/cm^2) for 5 min (gelatin/IL@Fe_3O_4+MW), the MW group was only treated with MW irradiation without microcapsules (MW only), the control group was untreated with MW irradiation without microcapsules (control). (d) MW heating curve of HepG2 cells with the samples in c. (e) Schematic illustration of MW heating. White and red represent the low and high temperature, respectively. Before the MW was irradiated, the charged ions (IL) were randomly dispersed inside the microcapsule. When once placed nearby a MW apparatus, the electric field could be help the charged ions to move accordingly. Under the action of MW, the microcapsules can heat up, which is induced through the friction and collision of molecules and ions with each other.

S2a in the Supporting Information) suggested the presence of Fe_3O_4 NPs (JCPDS card, No. 75−1609) in gelatin/IL@Fe_3O_4 microcapsules. After the final thermal destruction (Figure S2b in the Supporting Information), the residual percentages of weight of the gelatin, gelatin/IL and gelatin/IL@Fe_3O_4 microcapsules were 0, 2.59, and 17.95%, respectively. The higher residual content of the gelatin/IL and gelatin/IL@Fe_3O_4 microcapsules were certainly attributed to the IL and IL@Fe_3O_4, respectively.

To verify the potential of microcapsules in MW thermotherapy, microcapsules solution (50 mg/mL, 1 mL) was exposed to a MW irradiation at power density of 1.8 W/cm^2. Water, Fe_3O_4, saline, gelatin, and gelatin/Fe_3O_4 microcapsules were used as control groups. A rapid temperature increase of the gelatin/IL and gelatin/IL@Fe_3O_4 microcapsules when exposed to MW irradiation was reached to a high level (ΔT = 23.8 °C and ΔT = 24.1 °C, respectively), whereas water, Fe_3O_4, saline and gelatin groups showed much less temperature change (ΔT = 7.8 °C, ΔT = 7.9 °C, ΔT = 17.4, and 17.5 °C, respectively) (Figure 1e), suggesting that either Fe_3O_4 or gelatin/Fe_3O_4 microcapsules by itself did not affect the temperature elevation. IR thermal image of gelatin/IL@Fe_3O_4 microcapsules after MW irradiation at 1.8 W/cm^2 for 5 min also showed that the temperature of these microcapsules was significantly increased at more than 45 °C, which was high enough to kill cancer cells in vivo (inset of Figure 1e).

To demonstrate that gelatin/IL@Fe_3O_4 microcapsules could be used as MW susceptible materials and contrast agent in biomedical applications, we first evaluated their cytotoxicity characteristics. The hemolysis rate of microcapsules (250, 500, 1000, 5000 μg/mL) was evaluated. In Figure 2a show that all hemolysis rate at different concentrations were below 5%, indicating that the gelatin/IL@Fe_3O_4 microcapsules had good biocompatibility. It is found that the microcapsules have low erythrocyte membrane damaging effects (inset of Figure 2a). HepG2 cells were incubated with these microcapsules (25−1000 μg/mL) for cytotoxicity estimate on the basis of MTT assay. As shown in Figure 2b, when the cells were cultured with microcapsules for 24 h, no significant cytotoxicity of gelatin/IL@Fe_3O_4 microcapsules at concentrations of less than 1000

DOI: 10.1021/acsami.5b03230
ACS Appl. Mater. Interfaces 2015, 7, 13612−13619

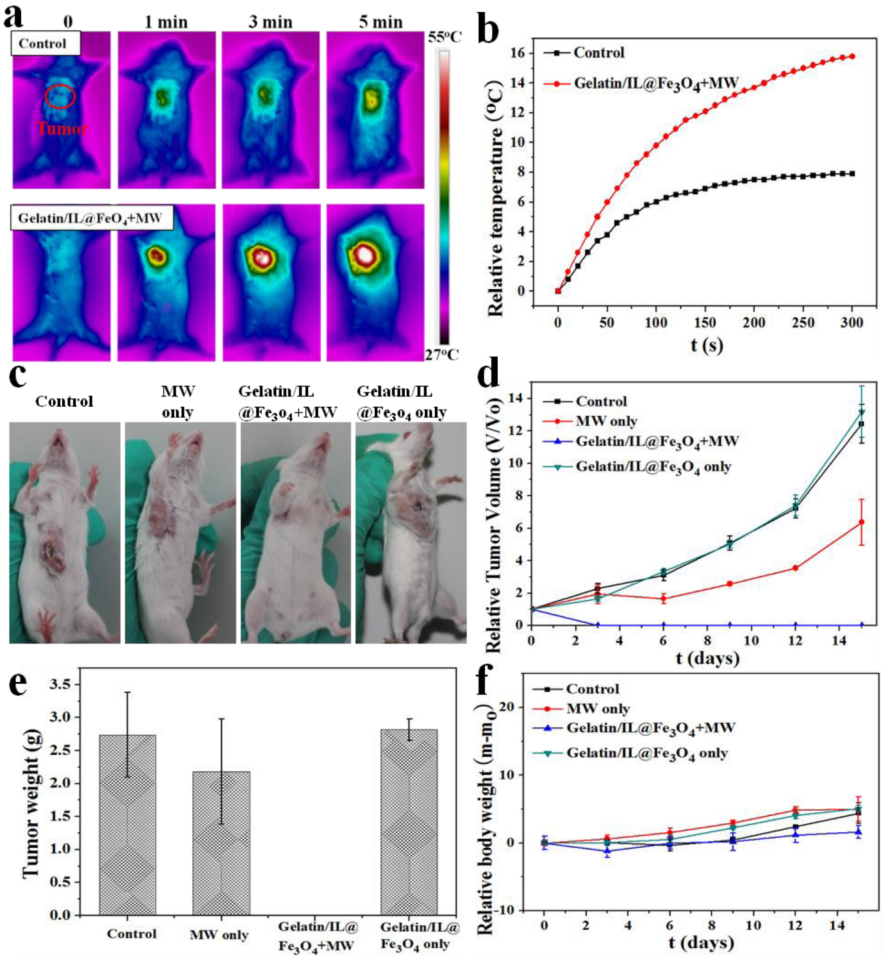

Figure 3. MW therapy using gelatin/IL@Fe_3O_4 microcapsules in vivo. (a) Infrared thermal images of saline injected and gelatin/IL@Fe_3O_4 microcapsules injected tumor-bearing mice at different time intervals under MW irradiation. (b) Temperature changes on tumors of mice under different treatments in a. (c) Representative photographs of mice bearing H22 tumors after various different treatments at day 16. (d) Tumor growth curves of tumor-bearing mice after various treatments. The tumor volumes were defined to their initial sizes. Error bars were based on standard deviations of 5 tumor-bearing mice per group. (e) Tumor weights of each group after excision. (f) Mean body weights of each group during the treatment.

μg/mL were observed. Moreover, as presented in Figure S3 in the Supporting Information, the activities of J744 cells or L929 cells treated with different concentrations of microcapsules were normal compared to control groups, indicating no obvious toxicity induced by microcapsules. These results indicated that these microcapsules were potentially suitable for biomedical applications.

To investigate the MW susceptible properties of our gelatin/IL@Fe_3O_4 microcapsules in vitro, we evaluated the viability of HepG2 cells after being mixed with gelatin/IL@Fe_3O_4 microcapsules under MW irradiation (450 MHz, 1.8 W/cm^2) for 5 min by MTT. As shown in Figure 2c, remarkably enhanced cell-killed effect was observed in HepG2 cells treated by microcapsules after MW exposure, compared to the control group and the MW only groups. Moreover, the temperature of gelatin/IL@Fe_3O_4 microcapsules can rapidly increase from 25 to 43.9 °C, whereas the MW only group shows a much lower temperature increase (Figure 2d), which was consistent with the results of Figure 1e.

MW irradiation-triggered heating involves two main mechanisms: dipolar polarization and ionic conduction.[36,39,40] The MW heating of IL is ascribed to the ionic conduction mechanism, which represents a much stronger heat generation capacity than the dipolar polarization.[3,9,12,43−45] The charged ions oscillate back and forth under the irradiation of the microwave, and collide with neighboring maters, leading to the generation of heat. Microcapsules have a compact shell structure, which can confine the oscillation of IL. As presented in Figure 2e, before the MW was irradiated, the charged ions (IL) were randomly dispersed inside the microcapsule. When the MW irradiation is applied, the oscillation of IL is confined in the microcapsules, leading to more serious friction and collision of molecules and ions than the free IL. Thus, efficient, rapid, and selective heating occurs in the microcapsules.

Then MW thermotherapy of gelatin/IL@Fe_3O_4 microcapsules on a H22 tumor mouse model was evaluated. Female ICR mice bearing H22 tumors were intratumorally injected with gelatin/IL@Fe_3O_4 microcapsules (200 mg/kg) and then subjected to the MW irradiation (1.8 W/cm^2, 5 min). Tumors treated with saline were used as control group. The temperature of tumor was monitored using an infrared thermal camera and fiber thermometers during MW irradiation, respectively. As shown in Figure 3a and b, the temperature of the tumor injected with gelatin/IL@Fe_3O_4 microcapsules can be rapidly increase to about 52 °C (ΔT = 15.8 °C) within 5 min under MW irradiation. However, control group showed a

DOI: 10.1021/acsami.5b03230
ACS Appl. Mater. Interfaces 2015, 7, 13612−13619

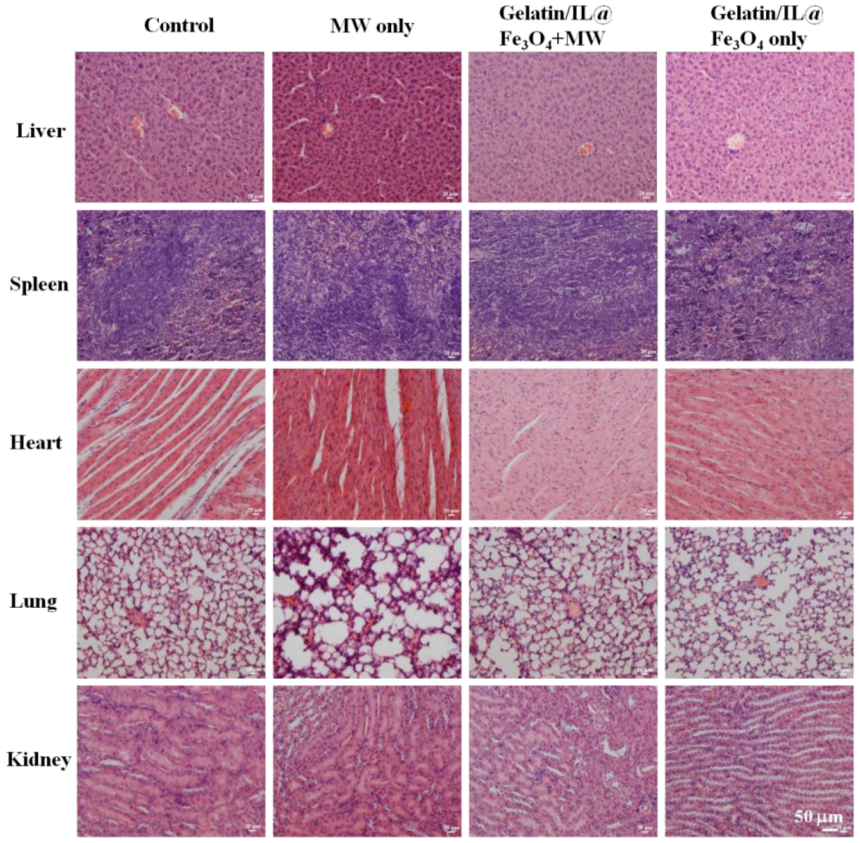

Figure 4. H&E stained organ slices collected from different groups of mice immediately after MW irradiation. The slices uncovered no apparent organ damage or abnormality. No obvious differences were observed between the control group and other groups.

limited temperature change, reaching final temperature at about 42 °C (ΔT = 7.8 °C) after MW irradiation (Figure 3a, b). This enhanced heating was due to the friction of molecules and/or ions with each other.[44,45] Irreversible cell injury occurs when cells sites are heated to high than 43 °C for several minutes, and cellular damage mainly centers on mitochondrial enzymes protein and protein coagulation of cytosolic, and nucleic acid protein complexes.[2−5] This result clearly revealed that gelatin/IL@Fe_3O_4 microcapsules can effectively kill the tumor cells in vivo by acting as a susceptible agent for MW therapy under MW irradiation.

Next, we evaluated in vivo MW thermo-therapeutic efficacy by observing the tumor growth in different groups of mice after MW exposure. Four groups of H22 tumor-bearing mice (five mice per group) were intratumorally injected with saline, gelatin/IL@Fe_3O_4 microcapsules, respectively. Tumor was then exposed to the MW irradiation at the ultra power density of 1.8 W/cm^2 for 5 min. The tumor size was measured by a vernier caliper every 3 days during the treatments. As shown in Figure 3c−e, it can be found that tumors treated with gelatin/IL@Fe_3O_4 microcapsules were completely ablated after MW irradiation, those treated with saline were showed rapid growth. Tumors in groups without MW irradiation showed similar growth speeds, suggesting that injection of saline and gelatin/IL@Fe_3O_4 microcapsules by itself would not affect the tumor growth. Our results further demonstrated that gelatin/IL@Fe_3O_4 microcapsules would be a powerful MW susceptible agent for effective tumor ablation.

To analyze the potential in vivo toxicity of gelatin/IL@Fe_3O_4 microcapsules, we carefully observed the behaviors of mice in our experiment. No mice died and without noticing side effects in the whole course of therapy. As presented in Figure 3f, the body weight had no significant difference between treatment groups and control group during the experiment, further suggesting that the thermotherapy has no acute fatal toxicity. Mice were sacrificed at 17 day for careful necropsy. Major organs of mice were fixed, embedded, sectioned and stained for histological examination. No noticeable sign of organ damage or inflammation lesion was observed in main organs (Figure 4) in these groups. Our results suggest that gelatin/IL@Fe_3O_4 microcapsules can be potentially used in clinical therapy.

At last, the potential in vivo MR imaging of gelatin/IL@Fe_3O_4 was also investigated. The magnetic properties of the synthesized gelatin/IL@Fe_3O_4 microcapsules were measured by vibrating sample magnetometry at room temperature. As presented in Figure S4 in the Supporting Information, the magnetization curve of gelatin/IL@Fe_3O_4 microcapsules was recorded at 1 T, and the magnetization recorded was 1.47 emu/g. The gelatin/IL@Fe_3O_4 microcapsules were rapidly attracted by the magnet, leaving the solution (inset of Figure 5a). T_2-weighted MR images of gelatin/IL@Fe_3O_4 microcapsules revealed the concentration-dependent darkening effect (inset of Figure 5a), with the relaxivity values of microcapsules measured to be 4.40 mg^{-1} mL s^{-1}. Then, the T_2 weighted MR imaging capability of gelatin/IL@Fe_3O_4 microcapsules was further evaluated in vivo. As shown in Figure 5b, a significant darkening with a T_2 signal intensity decrease of 79.27% in the T_2-weighted MR image was observed at the tumor site after gelatin/IL@Fe_3O_4 microcapsules were injected. These imply that as-prepared gelatin/IL@Fe_3O_4 microcapsules would be a promising candidate as a contrast agent in MR imaging for cancers. Combined with its functionality of MW therapy, it is

DOI: 10.1021/acsami.5b03230
ACS Appl. Mater. Interfaces 2015, 7, 13612−13619

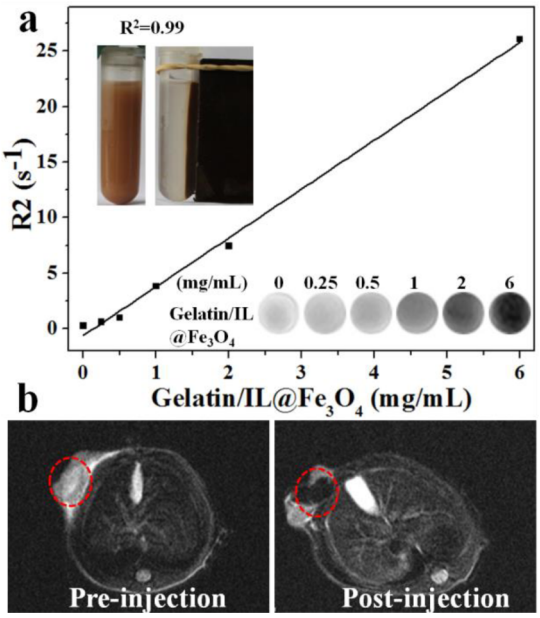

Figure 5. Magnetic properties of microcapsules and in vivo MR imaging. (a) The T_2 relaxation rates (r_2) of gelatin/IL@Fe_3O_4 microcapsules at different microcapsules concentrations. Inset: Photographs of gelatin/IL@Fe_3O_4 microcapsules in water with and without a magnet in the above, T_2-weighted MR images of gelatin/IL@Fe_3O_4 microcapsules at different microcapsules concentrations in the following. (b) In vivo T_2-weighted MR images of a tumor-bearing mice before and after injecting gelatin/IL@Fe_3O_4 microcapsules.

anticipated that the as-prepared gelatin/IL@Fe_3O_4 microcapsules would be a potential MW susceptible agent for simultaneous MR imaging and MW thermotherapy of cancers.

CONCLUSION

In summary, multifunctional microcapsules of gelatin shell/IL@Fe_3O_4 core were reported for the first time and used for MR imaging-guide MW thermotherapy. Obvious temperature increase of gelatin/IL@Fe_3O_4 microcapsules were found under MW irradiation, while pure water and saline showed minimal change. The MW susceptible properties of microcapsules make them an encouraging susceptible agent for MW cancer treatment. The result of MTT assay and hemolysis rate showed good biocompatibility and low erythrocyte membrane-damaging effects, respectively, revealing low cytotoxicity of these microcapsules. The as-prepared microcapsules can kill cell effectively in vitro and in vivo with exposure to MW irradiation, especially when the microcapsules were applied in MW thermotherapy in vivo, with 100% tumor elimination. No obvious toxicity was observed from the result of body weight during the treatment and the major of organs of histological investigations, and MW treatment for tumor with gelatin/IL@Fe_3O_4 microcapsules in vivo did not induced obvious side effect to the mice. Moreover, their efficient contrast enhancement in MR imaging in vivo was demonstrated. Therefore, these multifunctional microcapsules with excellent biocompatibility have great potential for MR imaging-guided MW thermotherapy.

ASSOCIATED CONTENT

Supporting Information

EDS, XRD, TG, cell viability of J744 cells or L929 cells, and magnetic hysteresis are included as Figures S1−S4. The Supporting Information is available free of charge on the ACS Publications website at DOI: 10.1021/acsami.5b03230.

AUTHOR INFORMATION

Corresponding Authors

*E-mail: mengxw@mail.ipc.ac.cn. Tel: (+86)10-82543521. Fax: (+86)10- 82543521.
*E-mail: zbhuang@scu.edu.cn.
*E-mail: haiboshao@aliyun.com.

Author Contributions

†Authors Q.D. and T.M. contributed equally. All coauthors have looked over this manuscript and approved the submission. X.M. conceived the project. X.M., Z.H., F.T., H.S., and K.X. designed the research. Q.D. and C.F. prepared the microcapsules and analyzed the basic properties. T.L. and J.R. conducted the in vitro hemolysis test and MTT assay experiments. C.F., T.M. ,and Q.D. created the mice model and did the animal experiments. T.M. conducted the histological study. X.M., T.M., and Q.D. wrote the paper.

Notes

The authors declare no competing financial interest.

ACKNOWLEDGMENTS

The authors acknowledge financial support from the National Hi-Technology Research and Development Program (863 Program) (No. 2013AA032201 and 2012AA022701), the National Natural Science Foundation of China (NSFC) (61171049, 31400854 and 81201814).

REFERENCES

(1) Ahmed, M.; Moussa, M.; Goldberg, S. N. Synergy in Cancer Treatment between Liposomal Chemotherapeutics and Thermal Ablation. *Chem. Phys. Lipids* **2012**, *165*, 424−437.
(2) Petros, R. A.; DeSimone, J. M. Strategies in the Design of Nanoparticles for Therapeutic Applications. *Nat. Rev. Drug. Discovery* **2010**, *9*, 615−627.
(3) Rock, C. L.; Doyle, C.; Demark-Wahnefried, W.; Meyerhardt, J.; Courneya, K. S.; Schwartz, A. L. Nutrition and Physical Activity Guidelines for Cancer Survivors. *CA-Cancer J. Clin.* **2012**, *62*, 243−274.
(4) Timmerman, R. D.; Bizekis, C. S.; Pass, H. I.; Fong, Y.; Dupuy, D. E.; Dawson, L. A. Local Surgical, Ablative, and Radiation Treatment of Metastases. *CA-Cancer J. Clin.* **2009**, *59*, 145−170.
(5) Chu, K. F.; Dupuy, D. E. Thermal Ablation of Tumours: Biological Mechanisms and Advances in Therapy. *Nat. Rev. Cancer* **2014**, *14*, 199−208.
(6) Cuenca, A. G.; Jiang, H.; Hochwald, S. N.; Delano, M.; Cance, W. G.; Grobmyer, S. R. Emerging Implications of Nanotechnology on Cancer Diagnostics and Therapeutics. *Cancer* **2006**, *107*, 459−466.
(7) Barreto, J. A.; O'Malley, W.; Kubeil, M.; Graham, B.; Stephan, H.; Spiccia, L. Nanomaterials: Applications in Cancer Imaging and Therapy. *Adv. Mater.* **2011**, *23*, H18−40.
(8) Huang, J.; Xu, J. S.; Xu, R. X. Heat-sensitive Microbubbles for Intraoperative Assessment of Cancer Ablation Margins. *Biomaterials* **2010**, *31*, 1278−86.
(9) Li, X.; Fan, W.; Zhang, L.; Zhao, M.; Huang, Z.; Li, W. CT-guided Percutaneous Microwave Ablation of Adrenal Malignant Carcinoma: Preliminary Results. *Cancer* **2011**, *117*, 5182−5188.
(10) Thomas, J. V.; Nagy, N. N. N.; Tatjana, G.-R.; Karen, K.; Thomas, L.; Nour-Eldin, A. Microwave Ablation Therapy: Clinical Utility in Treatment of Pulmonary Metastases. *Radiology* **2011**, *261*, 643−651.
(11) Ohlan, A.; Singh, K.; Chandra, A.; Dhawan, S. K. Microwave Absorption Behavior of Core-shell Structured Poly (3,4-ethylenedioxy

DOI: 10.1021/acsami.5b03230
ACS Appl. Mater. Interfaces 2015, 7, 13612−13619

thiophene)-barium Ferrite Nanocomposites. *ACS Appl. Mater. Interfaces* **2010**, *2*, 927−933.
(12) Wang, R.; Zhang, M.; Mujumdar, A. S.; Jiang, H. Effect of Salt and Sucrose Content on Dielectric Properties and Microwave Freeze Drying Behavior of Re-structured Potato Slices. *J. Food. Eng.* **2011**, *106*, 290−297.
(13) Hughes, M. D.; Lekitsch, B.; Broersma, J. A.; Hensinger, W. K. Microfabricated Ion Traps. *Contemp. Phys.* **2011**, *52*, 505−29.
(14) Palomaki, T. A.; Harlow, J. W.; Teufel, J. D.; Simmonds, R. W.; Lehnert, K. W. Coherent State Transfer between Itinerant Microwave Fields and a Mechanical Oscillator. *Nature* **2013**, *495*, 210−214.
(15) Ahmad, F.; Gravante, G.; Bhardwaj, N.; Strickland, A.; Basit, R.; West, K. Renal Effects of Microwave Ablation Compared with Radiofrequency, Cryotherapy and Surgical Resection at different Volumes of the Liver Treated. *Liver Int.* **2010**, *30*, 1305−1314.
(16) Dooley, W. C.; Vargas, H. I.; Fenn, A. J.; Tomaselli, M. B.; Harness, J. K. Focused Microwave Thermotherapy for Preoperative Treatment of Invasive Breast Cancer: a Review of Clinical Studies. *Ann. Surg. Oncol.* **2010**, *17*, 1076−1093.
(17) Fan, W.; Li, X.; Zhang, L.; Jiang, H.; Zhang, J. Comparison of Microwave Ablation and Multipolar Radiofrequency Ablation in vivo Using Two Internally Cooled Probes. *Am. J. Roentgenol.* **2012**, *198*, W46−50.
(18) Guan, W.; Bai, J.; Liu, J.; Wang, S.; Zhuang, Q.; Ye, Z. Microwave Ablation Versus Partial Nephrectomy for Small Renal Tumors: Intermediate-term Results. *J. Surg. Oncol.* **2012**, *106*, 316−321.
(19) Liu, Y.; Zheng, Y.; Li, S.; Li, B.; Zhang, Y.; Yuan, Y. Percutaneous Microwave Ablation of larger Hepatocellular Carcinoma. *Clin. Radiol.* **2013**, *68*, 21−26.
(20) Lubner, M. G.; Brace, C. L.; Hinshaw, J. L.; Lee, F. T. Microwave Tumor Ablation: Mechanism of Action, Clinical Results, and Devices. *J. Vasc. Interv. Radiol.* **2010**, *21*, S192−203.
(21) Sun, Y.; Cheng, Z.; Dong, L.; Zhang, G.; Wang, Y.; Liang, P. Comparison of Temperature Curve and Ablation Zone between 915- and 2450-MHz Cooled-shaft Microwave Antenna: Results in ex vivo Porcine livers. *Eur. J. Radiol.* **2012**, *81*, 553−557.
(22) Vogl, T. J.; Farshid, P.; Naguib, N. N.; Zangos, S. Thermal Ablation Therapies in Patients with Breast Cancer Liver Metastases: a Review. *Eur. Radiol.* **2013**, *23*, 797−804.
(23) Vogl, T. J.; Naguib, N. N.; Lehnert, T.; Nour-Eldin, N. E. Radiofrequency, Microwave and Laser Ablation of Pulmonary Neoplasms: Clinical Studies and Technical Considerations–Review Article. *Eur. J. Radiol.* **2011**, *77*, 346−357.
(24) Vollmer, C.; Redel, E.; Abu-Shandi, K.; Thomann, R.; Manyar, H.; Hardacre, C. Microwave Irradiation for the Facile Synthesis of Transition-metal Nanoparticles (NPs) in ionic liquids (ILs) from Metal-Carbonyl Precursors and Ru-, Rh-, and Ir-NP/IL Dispersions as Biphasic Liquid-liquid Hydrogenation Nanocatalysts for Cyclohexene. *Chemistry* **2010**, *16*, 3849−3858.
(25) Li, G.; Wang, L.; Li, W.; Ding, R.; Xu, Y. $CoFe_2O_4$ and/or Co_3Fe_7 Loaded Porous Activated Carbon Balls as a Lightweight Microwave Absorbent. *Phys. Chem. Chem. Phys.* **2014**, *16*, 12385−12392.
(26) Liu, T.; Pang, Y.; Zhu, M.; Kobayashi, S. Microporous Co@CoO Nanoparticles with Superior Microwave Absorption Properties. *Nanoscale* **2014**, *6*, 2447−2454.
(27) Liu, Z.; Cai, W.; He, L.; Nakayama, N.; Chen, K.; Sun, X. In vivo Biodistribution and Highly Efficient Tumour Targeting of Carbon Nanotubes in Mice. *Nat. Nanotechnol.* **2007**, *2*, 47−52.
(28) Druzhinina, T. S.; Hoeppener, S.; Schubert, U. S. Microwave-assisted Fabrication of Carbon Nanotube AFM Tips. *Nano Lett.* **2010**, *10*, 4009−4012.
(29) Bulmer, J. S.; Martens, J.; Kurzepa, L.; Gizewski, T.; Egilmez, M.; Blamire, M. G. Microwave Conductivity of Sorted CNT Assemblies. *Sci. Rep.* **2014**, *4*, 3762.
(30) Xu, J.; Liu, J.; Che, R.; Liang, C.; Cao, M.; Li, Y. Polarization Enhancement of Microwave Absorption by Increasing Aspect Ratio of Ellipsoidal Nanorattles with Fe_3O_4 cores and Hierarchical $CuSiO_3$ shells. *Nanoscale* **2014**, *6*, 5782−5790.
(31) Zhao, X.; Zhang, Z.; Wang, L.; Xi, K.; Cao, Q.; Wang, D. Excellent Microwave Absorption Property of Graphene-coated Fe Nanocomposites. *Sci. Rep.* **2013**, *3*, 3421.
(32) Gu, X.; Zhu, W.; Jia, C.; Zhao, R.; Schmidt, W.; Wang, Y. Synthesis and Microwave absorbing Properties of highly Ordered Mesoporous Crystalline $NiFe_2O_4$. *Chem. Commun.* **2011**, *47*, 5337−5339.
(33) Du, Q.; Fu, C.; Liu, T.; Li, L.; Ren, X.; Ren, J.; Huang, Z.; Liu, H.; Tang, F.; Meng, X. Gelatin Microcapsules for Enhanced Microwave Tumor Hyperthermia. *Nanoscale* **2015**, *7*, 3147−3153.
(34) Shi, H.; Liu, T.; Fu, C.; Li, L.; Tan, L.; Wang, J.; Ren, X.; Ren, J.; Wang, J.; Meng, X. Insights into a Microwave Susceptible Agent for Minimally Invasive Microwave Tumor Thermal Therapy. *Biomaterials* **2015**, *44*, 91−102.
(35) Fechler, N.; Fellinger, T. P.; Antonietti, M. "Salt templating": a Simple and Sustainable Pathway toward Highly Porous Functional Carbons from Ionic Liquids. *Adv. Mater.* **2013**, *25*, 75−79.
(36) Patel, D. D.; Lee, J. M. Applications of Ionic Liquids. *Chem. Rec.* **2012**, *12*, 329−355.
(37) Qian, G. J.; Wang, N.; Shen, Q.; Sheng, Y. H.; Zhao, J. Q.; Kuang, M. Efficacy of Microwave Versus Radiofrequency Ablation for Treatment of Small Hepatocellular Carcinoma: Experimental and Clinical Studies. *Eur. Radiol.* **2012**, *22*, 1983−1990.
(38) Ren, H.; Zhou, Y.; Liu, L. Selective Conversion of Cellulose to Levulinic Acid via Microwave-assisted Synthesis in Ionic Liquids. *Bioresour. Technol.* **2013**, *129*, 616−619.
(39) Smiglak, M.; Pringle, J. M.; Lu, X.; Han, L.; Zhang, S.; Gao, H. Ionic Liquids for Energy, Materials, and Medicine. *Chem. Commun.* **2014**, *50*, 9228−9250.
(40) Zhang, P.; Wu, T.; Han, B. Preparation of Catalytic Materials Using Ionic Liquids as the Media and Functional Components. *Adv. Mater.* **2014**, *26*, 6810−6827.
(41) Yang, L. J.; Ou, Y. C. The Micro Patterning of Glutaraldehyde (GA)-crosslinked Gelatin and its Application to Cell-culture. *Lab Chip.* **2005**, *5*, 979−984.
(42) Lakshminarayana, G.; Nogami, M. Proton Conducting Organic−inorganic Composite Membranes under Anhydrous Conditions Synthesized from Tetraethoxysilane/methyltriethoxysilane/trimethyl Phosphate and 1-butyl-3 methylimidazolium Tetrafluoroborate. *Solid State Ionics* **2010**, *181*, 760−766.
(43) Chen, Y.; Chen, H.; Sun, Y.; Zheng, Y.; Zeng, D.; Li, F. Multifunctional Mesoporous Composite Nanocapsules for Highly Efficient MRI-guided High-intensity Focused Ultrasound Cancer Surgery. *Angew. Chem. Int. Ed.* **2011**, *50*, 12505−12509.
(44) Liu, X.; Chen, H. J.; Chen, X.; Parini, C.; Wen, D. Low Frequency Heating of Gold Nanoparticle Dispersions for Non-invasive Thermal Therapies. *Nanoscale* **2012**, *4*, 3945−3953.
(45) Wang, X.; Chen, H.; Chen, Y.; Ma, M.; Zhang, K.; Li, F. Perfluorohexane- encapsulated Mesoporous Silica Nanocapsules as Enhancement Agents for Highly Efficient High Intensity Focused Ultrasound (HIFU). *Adv. Mater.* **2012**, *24*, 785−791.

DOI: 10.1021/acsami.5b03230
ACS Appl. Mater. Interfaces 2015, 7, 13612−13619